

Closing probabilities in the Kauffman model: an annealed computation.

U. Bastolla and G. Parisi

October 8, 2018

Department of Physics, University “La Sapienza”, P.le Aldo Moro 2, I-00185 Roma, Italy

Keywords: Disordered Systems, Genetic Regulatory Networks,
Random Boolean Networks, Cellular Automata

Abstract

We define a probabilistic scheme to compute the distributions of periods, transients and weights of attraction basins in Kauffman networks. These quantities are obtained in the framework of the annealed approximation, first introduced by Derrida and Pomeau. Numerical results are in good agreement with the computed values of the exponents of average periods, but show also some interesting features which can not be explained within the annealed approximation.

1 Introduction

Kauffman Networks are a disordered dynamical system. They were introduced in 1969 as a simplified model of the genetic regulatory system acting in cell differentiation [1]. The debate about cellular automata grew the interest of physicists about the model [2]. It was soon recognized [5] that it has deep analogies with a disordered system studied in statistical mechanics, the infinite range Spin Glass, whose properties had been investigated and understood in the immediately former years [3].

A configuration of the system consists of N binary variables, $\sigma_i = 0, 1$, $i = 1 \dots N$. In the biological metaphor, the variable σ_i represents the state of activation of the i -th gene in the cell.

The configuration space is provided of a metric structure through the Hamming distance (normalized to one), say the fraction of variables whose states are different between two configurations C and C' :

$$d(C, C') = \frac{1}{N} \sum_{i=1}^N \left(\frac{\sigma_i - \sigma'_i}{2} \right)^2. \quad (1)$$

The system is disordered in the sense that the dynamic is deterministic, but its rules are chosen at random at the beginning in the following way: for each gene i , K genes are extracted randomly to send a signal to it (the same gene can be extracted more than once); these are denoted by $j_l(i)$, $l = 1 \dots K$; for each gene i and each of the 2^K configurations of the signal it can receive, the value of the response function $f_i(\sigma_1 \dots \sigma_K)$ is extracted to be 0 with probability p and 1 with probability $1 - p$. The dynamic rules are then quenched and do not change during the evolution of the system.

At each time step the N variables are updated simultaneously, according to the signal received and to the response to that signal:

$$\sigma_i(t+1) = f_i(\sigma_{j_1(i)}, \dots, \sigma_{j_K(i)}). \quad (2)$$

In a more compact way, the evolution law can be put in the form $C(t+1) = \Phi_\eta(C(t))$, where C denotes a configuration of the dynamic variables and η a configuration of the dynamic rules.

Due to the fact that configuration space is finite, every trajectory ends up, after a transient time, on a periodic orbit, and configuration space is partitioned into a certain number of attraction basins of weight W_α , where the α labels the periodic orbit. So, as it is customary in the theory of disordered systems, three kinds of average have to be defined:

- The time average, which is equivalent to the average over a given limit cycle.
- The average over the same network, where different cycles have to be weighted with their own W_α .
- The average over different realizations of the network.

It was soon discovered that Kauffman Networks have two different kinds of dynamical behaviours: a *frozen* regime, when the average cycle length grows as a power of N , and a *chaotic* regime when it grows exponentially with N .

It is possible to characterize this transition as a phase transition and two order parameters have been found to describe it.

Derrida and Pomeau considered the average limit distance between configurations on two randomly chosen trajectories in the same network. They computed its value in the framework of the annealed approximation and found that it is zero in the frozen phase (in the limit of an infinite network: remember that the distance is defined as the fraction of different variables), while it is different from zero in the chaotic one [4, 8, 7].

Then Flyvbjerg introduced the concept of *stable core*, defined as the set of the variables that evolve to a constant state not depending on the initial configuration. The fraction of variables belonging to the stable core is 1 (in the limit of infinite N) in the frozen phase while is less than 1 in the chaotic phase [13].

The transitions described by these parameters take place at the same critical point, $p = p_c(K)$, where p_c is such that $2p_c(1 - p_c) = 1/K$ [4, 8, 7, 13].

Despite of the success of this approach, the connection between these order parameters and dynamical properties (of the kind of the average cycle length or the weights of attraction basins) is still lacking. This work is a contribute to fill in this gap.

In the second section we define the closing probabilities, which are the quantities that allow to compute the full cycle length and transient time distribution. Section 3 describes the annealed approximation, first introduced by Derrida and Pomeau [4], that here is used to compute the distribution of the overlap between different time configurations and the closing probabilities, whence we obtain the distribution of cycle lengths (section 4) and the distribution of attraction basins weights in the chaotic phase (section 5), which turn out to be the same as those obtained by Derrida and Flyvbjerg in the limit case $K \rightarrow \infty$ (the so called Random Map) [6]. Section 6 deals with the average number of cycles in a given network, which is computed in the chaotic phase, in the framework of the annealed approximation.

In section 7 numerical results are presented. This section is subdivided into three sub-sections: in the first one, data concerning the distribution of the overlap are shown; they support the validity of the annealed approximation, but only in some range of the temporal variables. In section 7.2 simulations about the closing probabilities are reported, which show deviations from the annealed approximation after an initial agreement. In section 7.3 we show the exponents which give the N behaviour of the average cycle length for different values of the parameter K ; there is a good agreement between our computations and the numerical results, but the distribution of cycle lengths that we measured is quite different from the predicted one.

In the last section we interpret the meaning of the approximation used and the discrepancies that we noticed with the simulations, and point out the direction of future work.

2 Closing probabilities

In the following, we will use the overlap $q(C, C') = 1 - d(C, C')$ to describe the metric of configuration space.

We will follow a stochastic strategy, with the aim to compute the probability distribution of the overlap $q(t, t')$ between the configurations $C(t)$ and $C(t')$, $t' > t$, on the same trajectory. It is convenient to consider only trajectories not yet closed at time $t' - 1$, so what we actually want to compute is a conditional probability, that we denote by the symbol $F_N(t, t'; q)$.

We define the closing probability $\pi_N(t, t')$ as the probability to find $q(t, t') = 1$, which means that the two configurations are equal, over a trajectory not yet closed at time $t' - 1$:

$$\pi_N(t, t') = P \{q(t, t') = 1 \mid q(t_1, t_2) < 1, t_1 < t_2 < t'\}. \quad (3)$$

We will have also to deal with the integral closing probability, $\tilde{\pi}_N(t)$, which is the probability that a trajectory not yet closed closes at time t regardless of the length of the cycle reached, $\tilde{\pi}_N(t) = \sum_l \pi_N(t - l, t)$.

Then it is easy to compute $F_N(t)$, the probability that a trajectory has not yet closed at time t . It satisfies the equation $F_N(t + 1) = F_N(t) (1 - \tilde{\pi}_N(t))$, whence, in the limit of large systems, introducing a continuous time variable, and using the fact that $\tilde{\pi}_N(t)$ is small even at times when nearly every trajectory has closed, one finds the simple expression

$$F_N(t) = \exp \left(- \int_0^t \tilde{\pi}_N(\tau) d\tau \right), \quad (4)$$

so that the probability to find a trajectory that, after a transient time t , reaches a cycle of length l , is given by

$$P \{T = t, L = l\} = \exp \left(- \int_0^{t+l} \tilde{\pi}_N(\tau) d\tau \right) \pi_N(t, t + l). \quad (5)$$

3 Annealed approximation: the overlap distribution

The goal to compute the overlap distribution becomes easier if one can reduce the dynamics of the overlap to a stochastic process.

We can treat Kauffman model as a stochastic process by extracting the values of the response functions not at the beginning, but every time a variable receives a signal that it had never received, and using the values already extracted every time the same signal comes back. Note that, if every gene receives signals from the whole system, we have not to worry about this last eventuality, which never occurs before the trajectory closes. In this case the annealed approximation that we are going to define is exact. This case corresponds to the limit of infinite K and is known as the Random Map model, studied analytically by

Derrida and Flyvbjerg [6]. In this work, we generalize their results to finite K values, in the framework of the annealed approximation.

Thus, in order to compute the overlap between two configurations, for every gene we distinguish two cases: either the gene received the same signal $S_i(t)$ at the two previous time steps, and so it will be in the same state, or it didn't:

$$q(t+1, t'+1) = \frac{1}{N} \sum_i \delta_{S_i(t)S_i(t')} + \frac{1}{N} \sum_i \left(1 - \delta_{S_i(t)S_i(t')}\right) \delta_{f(S_i(t))f(S_i(t'))}. \quad (6)$$

Now, the annealed approximation consists in this: we extract at random *at every time step* all the connections in the network, keeping memory only of the minimal information about the overlap $q(t, t')$, so that the probability that the two signals $S_i(t)$ and $S_i(t')$ are the same is $q(t, t')^K$; if they are not equal, we extract at random the values of the response function, and they will be equal with probability $1 - \rho$, where $\rho = 2p(1 - p)$ [4].

Derrida and Pomeau introduced the annealed approximation in order to obtain the equations for the evolution of the average Hamming distance between two randomly chosen configurations; we will use it in order to treat the overlap as a Markovian stochastic process, and so to compute the closing probabilities. We will argue later from our simulations that the overlap distribution obtained through the annealed approximation is very close to the quenched one.

It is not possible, using this kind of approximation, to impose the condition that the trajectory where we measure $q(t, t')$ was not closed at time $t' - 1$: we can only impose that it did not close on a cycle of length $l = t' - t$. As we shall see, this fact is likely to be the source of the main discrepancies between the annealed approximation and our simulations.

If we impose this condition, we obtain the master equation

$$P_N(t+1, t+l+1; q_n) = \binom{N}{n} \frac{\sum_{m=0}^{N-1} P_N(t, t+l; q_m) (\gamma(q_m))^n (1 - \gamma(q_m))^{N-n}}{1 - P_N(t, t+l; 1)}, \quad (7)$$

where $q_m = m/N$ and

$$\gamma(x) = (1 - \rho) + \rho x^K. \quad (8)$$

Given an initial distribution $P_N(0, l; q)$, the process defined by (7), which is ergodic because we exclude the overlap $q = 1$, evolves to a stationary distribution independent on both t and l , which appears only in the initial distribution but not in the transition probability.

We look for a stationary distribution \tilde{P}_N in an exponential form,

$$\tilde{P}_N(q = x) = C_N(x) e^{-N\alpha(x)}. \quad (9)$$

In the limit $N \rightarrow \infty$ we can use continuous variables, transform the sum into an integral and apply the saddle point method to perform it, obtaining the following selfconsistence equations for the unknown functions $\alpha(x)$ and $q(x)$ (the last one is the saddle point of the integral for a given value of x):

$$\alpha'(q(x)) - \gamma'(q(x)) \left(\frac{x}{\gamma(q(x))} - \frac{1-x}{1-\gamma(q(x))} \right) = 0 \quad (10)$$

$$\alpha(x) = \alpha(q(x)) + x \log \left(\frac{x}{\gamma(q(x))} \right) + (1-x) \log \left(\frac{1-x}{1-\gamma(q(x))} \right), \quad (11)$$

with the condition $q(x) < 1$.

Deriving the first equation and inserting the result in the second one we get a non-local transcendent equation for the function $q(x)$:

$$\gamma'(q(x)) \left(\frac{x}{\gamma(q(x))} - \frac{1-x}{1-\gamma(q(x))} \right) = \log \left(\frac{q(x)}{1-q(x)} \right) - \log \left(\frac{\gamma(q(q(x)))}{1-\gamma(q(q(x)))} \right). \quad (12)$$

We were not able to solve this equation, so we had to solve numerically a discrete version of it in order to obtain the exponent of the closing probability, $\alpha(1)$.

Before to turn to this point, however, there are some important features of the overlap distribution that can be easily understood.

Deriving (11), we can see that the point $Q(t)$ where the overlap distribution is concentrated satisfies the equation

$$Q(t+1) = \gamma(Q(t)), \quad (13)$$

which, at stationarity, becomes

$$Q^* = \gamma(Q^*) = 1 - \rho + \rho Q^{*K}. \quad (14)$$

This equation was first derived by Derrida and Pomeau as a mean field solution of the annealed model [4]. The condition $\gamma'(1) = K\rho = 1$ separates parameter space in two different regions:

- $K\rho \leq 1$: *frozen phase*. The only fixed point of the map (13) is $Q^* = 1$. This implies, as we shall see, that $\alpha(1)$ goes to zero and the typical cycle length increases less than exponentially with system size.
- $K\rho > 1$: *chaotic phase*. The fixed point $Q^* = 1$ becomes unstable (moreover, it would give raise to a negative variance) and the overlap is concentrated around another fixed point of (13), $Q^* < 1$. In this case $\alpha(1)$ is finite and the typical cycle length increases exponentially with system size.

The variance of the distribution can also be easily obtained, in the Gaussian approximation, deriving (11) twice and imposing the saddle point condition. One finds that the variance multiplied by N , $V(t)$, follows the recursive equation

$$V(t+1) = (\gamma'(Q(t))^2 V(t) + Q(t+1)(1-Q(t+1))), \quad (15)$$

whose fixed point is

$$V^* = \frac{Q^*(1-Q^*)}{1 - (\gamma'(Q^*))^2} \quad (16)$$

It is apparent that the stationary overlap distribution is a non binomial one: the presence of correlations between the genes are made evident by the fact that V^* is larger than $Q^*(1-Q^*)$. Moreover, it is also easy to see that $\alpha'(1)$ is approximately equal to ρK and does not diverge, while in the binomial distribution it does.

On the other hand, when K tends to infinity destroying the correlations between consecutive overlaps, the stationary overlap distribution becomes a binomial one and Q^* tends exponentially to $1 - \rho$.

In the frozen phase, when $\gamma'(1) \leq 1$, $Q^* = 1$ is the true solution of equation (14), and $\alpha(1)$ vanishes or, to say better, is of order $1/N$.

It is important to see how the term of $O(1)$ vanishes with time: to see that, let us see what happens at the critical point $\rho = 1/K$.

The evolution of the most probable overlap at the critical point, for $K > 1$, is such that, introducing a continuous time variable,

$$Q'(t) = \frac{1}{K}(Q-1)^2 \sum_{i=1}^{K-1} (K-1-i)Q^i, \quad (17)$$

and the asymptotic behaviour in t is

$$1-Q \propto \left(\frac{(K-1)t}{2} \right)^{-1}. \quad (18)$$

Let's now turn to the numerical computation of the exponent of the closing probability, $\alpha(1)$.

We have to use the discrete variables $q_i = i/N$; moreover, in place of the stationary state equation, we consider the evolution of the exponent of the overlap distribution, $\alpha_t(\{q_i\})$ (we omit to specify the dependence on l , which appears only in the initial condition $\alpha_0(\{q_i\})$).

Neglecting the normalization factor, in the master equation, we get the following map for the evolution of $\alpha_t(q_i)$:

$$\alpha_{t+1}(q_i) = q_i \log(q_i) + (1-q_i) \log(1-q_i) + \min_{j < N} (\alpha_t(q_j) - (q_i) \log(\gamma(q_j)) - (1-q_i) \log(1-\gamma(q_j))), \quad (19)$$

This map does not have a fixed point $\{\bar{\alpha}(q_i)\}$, as it can be seen numerically: for instance, $\alpha_t(1)$ reaches a minimum at a certain time and then increases uniformly.

This increase is not in contradiction with the existence of a stationary distribution; in fact equation (19) misses the normalization factor $(1 - P(1))^{-1}$, and so the probability computed by means of it has to decrease when the exact probability has reached the stationary value.

The increment is of order $O\left(\frac{1}{N^2}\right)$, because, after $Q_N(t)$ reaches its stationary value Q^* , $\alpha(Q_N^*)$ grows of a term of that order due to the difference, $O\left(\frac{1}{N}\right)$, between Q_N^* and $\gamma(Q_N^*)$, so it is not important because we also miss terms of order $\frac{1}{N}$ in the saddle point approximation. In our algorithm, we decided to get the function $\alpha_t(q_i)$ at the time when $\alpha_t(1)$ reaches its minimum value.

There is another finite N effect in our numerical calculation: because of the condition $j < N$ (this means that the overlap $x_j = 1$ cannot be taken as a starting point), the stationary value of $\alpha_N(x_i)$ decreases with N . In fact, the larger is N , the lower can be the minimum in (19), and the effect, of order $1/N$, is important especially for $i = N$, because in this case in the stationary state the minimum in (19) would be attained for $j = N$.

The finite size effects become more relevant at the critical line $\rho = 1/K$. As a discretization effect, the most likely value of the annealed distribution is not $Q^* = 1$, because the corresponding value $j = N$ in the equation (19) is not allowed, and at stationarity $\alpha(x_i)$ has a minimum for $Q_N^* = 1 - \epsilon_N$, where ϵ_N is $O\left(\frac{1}{\sqrt{N}}\right)$, so that $\gamma(Q_N^*) - Q_N^*$ is of order $O\left(\frac{1}{N}\right)$.

Actually, in the frozen phase the equation (19) is not more a good approximation, because then we are not allowed to neglect $P(1)$ in the denominator of equation (7). We keep it in the complete form and obtain the equation for the first moments of the distribution:

$$(1 - \rho) + \rho \langle q^K \rangle = \langle q \rangle (1 - P(1)) + (P(1)), \quad (20)$$

whence, at the critical point, neglecting terms of order $\langle (q - \langle q \rangle)^3 \rangle$ and $(1 - \langle q \rangle)^3$, one gets

$$P = \frac{K - 1}{2} \left(1 - \langle q \rangle + \frac{V}{N(1 - \langle q \rangle)} \right). \quad (21)$$

This suggests that both $P(1)$ and $1 - \langle q \rangle$ are of order $1/\sqrt{N}$. Combining this fact with the previous results, one finds in the critical line an asymptotic closing probability of the form

$$\pi_N(t, t') \propto \frac{1}{\sqrt{N}} \exp\left(\frac{-4N}{(K - 1)t^2}\right), \quad (22)$$

while in the chaotic phase we find an exponential behaviour:

$$\pi_N(t, t') \propto e^{\alpha(1)N}, \quad (23)$$

provided that the smallest time t is large enough for the overlap to reach the stationary distribution.

4 Period distribution within the Annealed Approximation

We now use the closing probabilities obtained in the previous section to compute the asymptotic distribution of transient times T and cycle lengths L .

In the chaotic phase, inserting the expression for the asymptotic closing probability into the equation (5), we obtain

$$\text{Prob} \{T = t, L = l\} \simeq \exp\left(-\frac{1}{2}(t+l)^2 e^{-\alpha N}\right) e^{-\alpha N}, \quad (24)$$

(from now on, we will shortcut $\alpha(1)$ with α).

So, for finite K , we obtain the same form of the distribution as in the Random Map Model, differing only in the value of α .

Introducing the continuous variables $x = t/\tau$ and $y = l/\tau$, with

$$\tau = e^{\frac{1}{2}\alpha N}, \quad (25)$$

the period and transient distribution becomes a continuous distribution with density

$$f(x, y) = e^{-\frac{1}{2}(x+y)^2}. \quad (26)$$

While the form of the distribution predicted by the annealed approximation is not confirmed by our simulations, the N behaviour of the time scale τ is in good agreement with the results of the simulations, as it is shown by figure 12 where we compare the value of α obtained by the iteration of equation (19) with twice the exponent of the average cycle length and transient time or with the exponent of the variance of the period obtained by a fit of experimental data, for some K value. Other numerical results will be presented later.

In the frozen phase α vanishes, and the average cycle length grows as a power of N . The closing probability, for $K \neq 1$, is given by

$$\pi_N(t, t+l) \propto \frac{1}{(K-1)\tau} \exp\left(-\left(\frac{2\tau}{t}\right)^2\right), \quad (27)$$

where the time-scale at the critical point is given by

$$\tau = \sqrt{N/(K-1)}. \quad (28)$$

This suggests a kind of universality of the critical line in the Kauffman model: the time scale of the dynamics diverges always as the square root of the number of the elements (except for the case $K = 1$, where the variance in the Gaussian approximation diverges linearly with t , thus destroying the validity of the approximation, and our method fails).

It is easy to see that the exponent α of the closing probability vanishes quadratically when ρ approaches to the critical point (except for the case $K = 1$). In fact, putting $\rho = \rho_c + \epsilon$, one finds

$$Q^* = 1 - \frac{2K}{K-1}\epsilon + o(\epsilon), \quad (29)$$

$$\alpha \approx \frac{1}{2} \frac{(1 - Q^*)^2}{V} = \frac{(2K)^2}{K-1} \epsilon^2 + o(\epsilon^2) \quad (30)$$

(of course these expressions are not valid in the limit case of infinite K , where the overlap distribution is a binomial one with mean value $1 - \rho$ and α is equal to $-\log(1 - \rho)$).

5 Distribution of weights

In Kauffman networks configuration space breaks into a number of limit cycles with their own attraction basins. The statistical distribution of the weights of such basins, W_α (the rate of the number of configurations in the basin to the total number), has been computed in the limit cases $K = 1$ and $K = \infty$ by Derrida and Flyvbjerg [6] and Flyvbjerg and Kjaer [11] respectively.

In the framework of the annealed approximation it is possible to obtain this distribution for every value of the parameters, at least in the chaotic phase: in this case, it turns out to be the same distribution computed in [6] for the Random Map.

Following [6], it is convenient to start computing the quantities

$$\bar{Y}_p = \sum_{\alpha} \bar{W}_{\alpha}^p, \quad (31)$$

that are the moments (of order $p - 1$) of the probability to find a basin of weight W . They can be computed by noting that they represent the probability that p configurations chosen at random ultimately meet.

In the framework of the annealed approximation, one finds that these quantities do not depend, in the chaotic phase and in the limit $N \rightarrow \infty$, on the parameter τ which gives the cycle length time scale, and have the same values computed by Derrida and Flyvbjerg for the case of the Random Map.

To be more concrete, let's calculate \bar{Y}_2 . We must generate randomly two trajectories on the same network. We extract the first one and follow it till the time T_1 when it closes on itself, as we have done in the previous section; then we generate another "replic" of the system and we study the overlap $q_{12}(t_1, t_2)$ between the configuration at time t_1 on the first trajectory and the one at time t_2 on the second one.

We define the closing probability of the second trajectory on the first one as the probability that $q_{12}(t_1, t_2)$ is equal to 1, with the condition that the first trajectory is composed of

T_1 different configurations, the second of $t_2 - 1$ different ones and none of them has met the first trajectory before time t_2 (we express this condition by the symbol $O(T_1, t_2)$):

$$\pi_N^{(2)}(T_1; t_1, t_2) = P \{q_{12}(t_1, t_2) = 1 | O(T_1, t_2)\}. \quad (32)$$

The probability that the second trajectory meets the first one after T_2 time steps is then

$$F_N^{(2)}(T_1, T_2) \tilde{\pi}_N^{(2)}(T_1; T_2), \quad (33)$$

where $\tilde{\pi}_N^{(2)}(T_1; t_2)$ is the integral closing probability, say the sum over t_1 of $\pi_N^{(2)}(T_1; t_1, t_2)$, and $F_N^{(2)}(T_1, T_2)$ is the probability that the second trajectory is composed of T_2 different configurations and they don't touch the first trajectory before time T_2 . One has, in the limit of continuous time variables,

$$F_N^{(2)}(T_1, T_2) = \exp \left(- \int_1^{T_2-1} (\tilde{\pi}_N^{(2)}(T_1; t) + \tilde{\pi}_N^{(2)}(t)) dt \right), \quad (34)$$

and

$$\bar{Y} = \sum_{T_1, T_2} F_N(T_1) F_N^{(2)}(T_2, T_1) \tilde{\pi}_N(T_1) \tilde{\pi}_N^{(2)}(T_2; T_1), \quad (35)$$

where $\tilde{\pi}_N(t)$ and $F_N(t)$ are respectively the integral closing probability and the opening probability for only one trajectory, as defined in the second section.

In the framework of the annealed approximation, we can imagine that the overlap $q_{12}(t, 0)$ between the initial configuration of the second trajectory and a given configuration of the first one is a binomial variable, and that the distribution of $q_{12}(t+1, 1)$ is obtained from it through the annealed evolution equation.

In this hypothesis, asymptotically in t_1 and t_2 , the closing probability in the chaotic phase is given by $\pi_N^{(2)}(T_1; t_1, t_2) = 1/\tau^2$, where $\tau = \exp(\alpha N/2)$ is the cycle length time scale.

Operating the substitutions $x = T_1/\tau$, $y = T_2/\tau$ and transforming to continuous variables, one then finds, for large values of τ ,

$$\bar{Y}_2 \simeq \int_0^\infty \int_0^\infty x^2 e^{-\frac{(x+y)^2}{2}} dx dy = 2/3, \quad (36)$$

which is independent on τ and is the same result of [6].

This computation generalizes easily to an arbitrary number of trajectories, and in this way one finds for everyone of the Y_p the same value obtained by Derrida and Flyvbjerg for the Random Map; so one can argue that $f(W)$, which has the meaning that $f(W)dW$ is the average number of cycles with weight between W and $W + dW$, is given, in the chaotic phase and in the framework of the annealed approximation, by the same expression valid in the Random Map model:

$$f(W) = \frac{1}{2}W^{-1} (1 - W)^{-1/2}. \quad (37)$$

To compare this prediction with numerical data, we have pursued the simulations performed by Derrida and Flyvbjerg [5] relatively to \bar{Y}_2 for $K = 3$, doubling the size of the maximum system simulated. For each system size we generated 10000 sample networks and two configurations at random on each of them and we measured Y_2 as the probability that they end up on the same cycle, as it was done in [5].

In this way we obtained a curve of Y versus N which reaches a minimum value of $Y = 0.590$ at $N = 40$ and then increases with N . The largest system that we could simulate ($N = 100$) looks to be still far from having attained the stationary value, so we are unable to say if it agrees with the annealed prediction $Y = 2/3$, but it is very close to that value (figure 1).

We measured also the histogram of the probability to find a cycle of weight W . Figure 2 compares the histogram obtained generating at random 1000 networks with $K = 3$ and $N = 50$ and simulating 250 trajectories on each of them with the one computed using (37), which is valid in the infinite N limit. The agreement, as it is possible to see, is not so bad.

6 Average cycle number

In this section we aim to compute the average number of cycles in a network, a quantity introduced by Kauffman to represent, in his biological metaphor, the typical number of possible cell types for a genome of given length. This quantity is difficult to observe in the simulations, because one must consider also cycles of very small weight, and has been computed only for the Random Map (infinite K , $\rho = 1/2$; [6]).

For this purpose, we have to compute the distribution of the overlap between a configuration at time t and the initial configuration, $P_N(0, t; q)$, which plays the role of the initial distribution for the stochastic process defined by the master equation (7).

It is easy to generalize the annealed approximation in order to get the transition probability of the joint distribution of the overlaps $q(0, t)$ and $q(t - 1, t)$: every gene remains at time $t + 1$ in the same state it was at the previous step with probability $\gamma(q(t - 1, t))$, where $\gamma(x)$ is defined in the previous section (8).

If the genes unchanged are Nz of the genes whose state was the same in the initial configuration and $N(q(t, t + 1) - z)$ of the other genes, the overlap $q(0, t + 1)$ is given by $1 - q(0, t) - q(t, t + 1) + 2z$. One then obtains the transition probability

$$P \{q(0, t + 1) = x_0, q(t, t + 1) = x_1 \mid q(0, t) = q_0, q(t - 1, t) = q_1\} = \binom{Nx_0}{Nz} \binom{N(1-x_0)}{N(x_1-z)} (\gamma(q_1))^{Nx_1} (1 - \gamma(q_1))^{N(1-x_1)}, \quad (38)$$

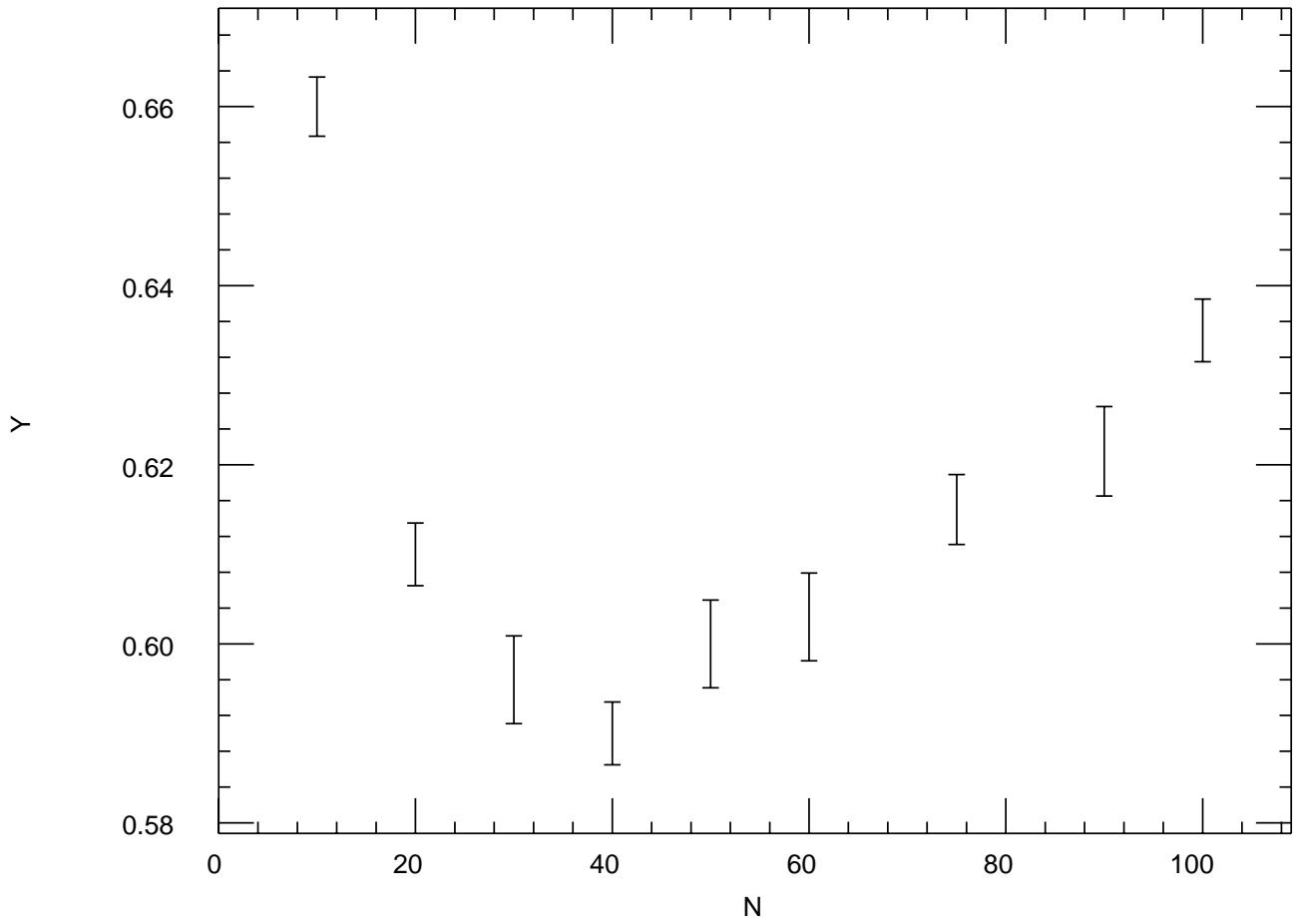


Figure 1: \bar{Y}_2 versus N in networks with $K = 3$. The annealed prediction is $\bar{Y}_2 = 0.6$.

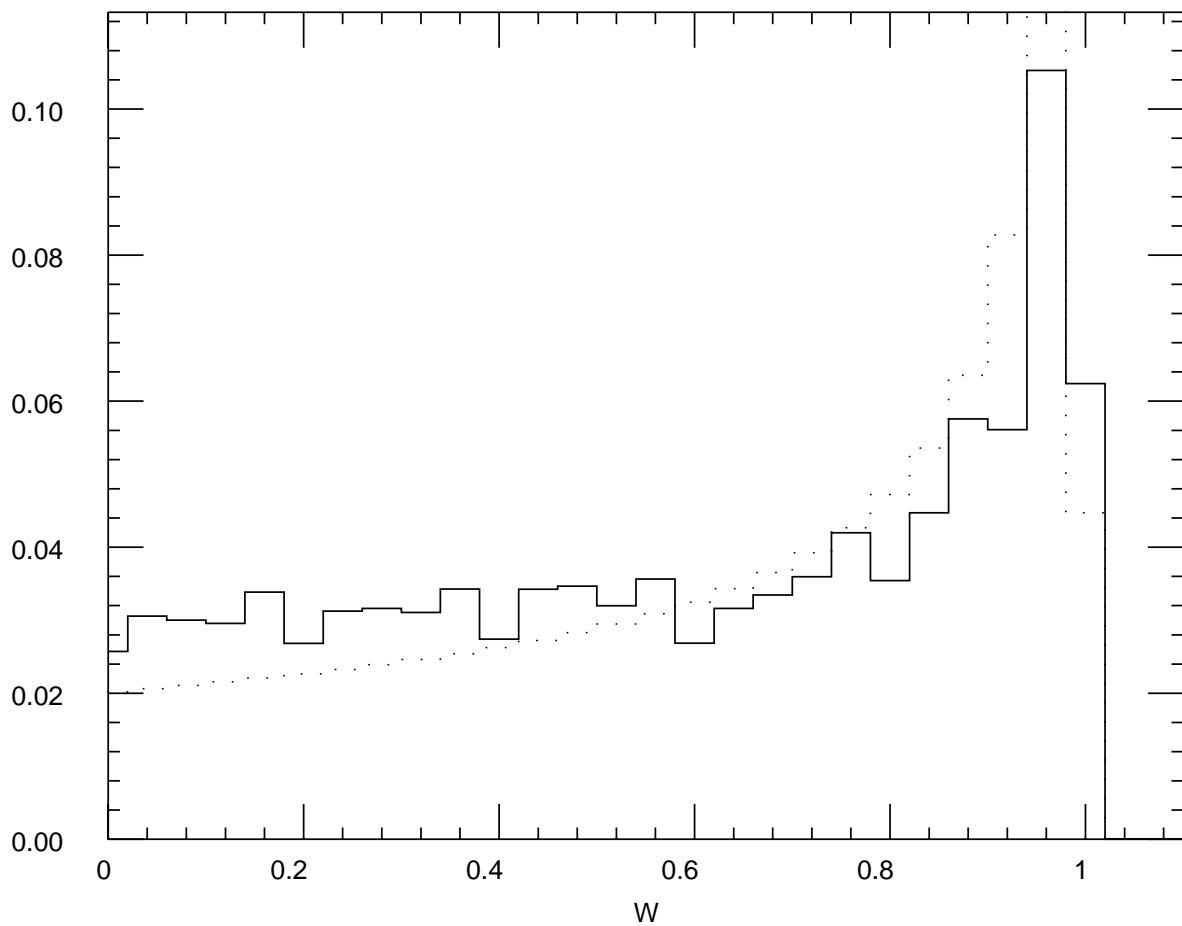


Figure 2: *Histogram of the probability to find a cycle of weight W in networks with $K = 3$ and $N = 50$, obtained simulating 1000 networks and 250 trajectories on each of them. The dotted line is the same thing, computed in the framework of the annealed approximation.*

with

$$z = \frac{1}{2}(x_1 + x_0 + q_0 - 1), \quad (39)$$

and with the bounds

$$|1 - (x_0 + x_1)| \leq q_0 \leq 1 - |x_0 - x_1|. \quad (40)$$

At time $t = 1$, the variables $q(0, t)$ and $q(t - 1, t)$ coincide and their distribution is a binomial one, but the correlations disappear after 2 time steps, at least in the Gaussian approximation, and the stationary joint distribution factorizes into the stationary distribution of $q(t - 1, t)$, that we met in the previous section, and a binomial distribution of mean value $1/2$. The most likely value of $q(0, t)$ is always $1/2$, even before that the stationary distribution has been reached, and the exponential part of the closing probability $\pi_N(0, t)$ (the probability to have $q(0, t) = 1$) is always $1/2^N$, but the prefactor is different from 1, in the initial steps. As usual, this can be seen putting the distribution in the exponential form and performing the integral with the saddle point method.

The average number of cycles of length l is related to the probability $P(l)$ to find a configuration belonging to a cycle of length l by the obvious formula

$$\bar{n}_l = \frac{2^N}{l} P\{L = l, T = 0\}. \quad (41)$$

In the framework of the annealed approximation, using the results of section 4 about period and transient distribution and the fact that $\pi_N(0, l) = 1/2^N c_l$ one finds, in the chaotic phase,

$$\bar{n}_l = \frac{c_l}{l} \exp\left(-\frac{1}{2} \frac{l^2}{\tau^2}\right). \quad (42)$$

Summing over l one gets the average number of cycles in a network. Apart from systems at the critical point, c_l is a quantity of order 1, and tends to 1 when l grows; so, substituting c_l by 1 and transforming the sum into an integral, one finds, asymptotically in τ , the following behaviour:

$$\sum_{l=1}^{2^N} \bar{n}_l \approx \log \tau = \frac{1}{2} \alpha N, \quad (43)$$

where α is the exponent of the stationary closing probability introduced in the previous section.

This formula is valid only in the chaotic phase: in the frozen phase, where α cancels, we are not allowed to put c_l to 1.

For instance, for $l = 2$ one finds

$$\pi_N(0, 2) = \frac{1}{2^N} \int e^{-Nf(x)} (x(1-x))^{-1/2} \frac{dx}{\sqrt{2\pi/N}}, \quad (44)$$

where

$$f(x) = x \log(x) + (1-x) \log(1-x) - x \log(\gamma(x)) - (1-x) \log(1-\gamma(x)). \quad (45)$$

($\gamma(x)$ is defined in (8)). The function $f(x)$ is concentrated around the same point Q^* around which it is concentrated the stationary distribution of the overlap, *i.e.* the solution of the equation $Q^* = \gamma(Q^*)$. The saddle point method with Gaussian corrections yields the result

$$\pi_N(0, 2) = \frac{1}{2^N} (1 - \gamma'(Q^*))^{-1}, \quad (46)$$

but at the critical point $\gamma'(Q^*)$ is equal to 1, so one has to go beyond Gaussian corrections and finds

$$\pi_N(0, 2) \propto \frac{1}{2^N} N^{1/6}. \quad (47)$$

7 Numerical tests of the Annealed Approximation

All simulations reported in this section are referred to Kauffman Networks with unbiased response functions, *i.e.* the parameter ρ is fixed at the value 0.5, and we will no longer mention it.

Our numerical analysis of the overlap distribution confirms the validity of the annealed approximation in some range of the time variables and reveals deviations from it in some other range, so that the period distribution turns out to be different from the one predicted by the annealed approximation, while the time-scale of the period and the first moment of the distribution of the weights are in good agreement with our computation.

7.1 Overlap distribution

We measured the overlap $q(t, t+l)$ on the subset of the trajectories not yet closed at time $t+l-1$, in order to sample with the conditional probability defined in section 2. In this way we also eliminate the "deterministic noise" due to the periodicity of the orbits.

For each value of the parameters, we generated 20'000 sample networks and on each of them we simulated a trajectory measuring the overlap $q(C(t), C(t+l))$ till the time when the trajectory closed. So we obtained the histogram of the overlap $q(t, t+l)$ for chosen values of the temporal distance l and t large enough to suppose that the distribution is stationary.

From the annealed approximation we expect the stationary distribution not to depend on l , but in fact we could observe different behaviours for different l values. So the data analysis is rather complex since for every point (K, ρ) in parameter space three variables, N , t and l , are involved and different limits, *e.g.* N large at fixed t and l or t and l large at fixed N , may give different behaviours.

We are interested to the exponential part of the stationary distribution, and we estimate it through the formula

$$\alpha_l(q) \approx \frac{1}{N} \left(-\frac{1}{2} \log N - \log P_{NI}(q) \right), \quad (48)$$

in which the factor $1/\sqrt{N}$ coming from the Stirling expansion of the binomial coefficient has been taken into account (actually, we use this formula only for $0.1 \leq q \leq 0.9$, while for $q = 0$ and 1 we don't subtract the term with $\log N$ and we interpolate linearly for intermediate values of q).

The function of q so obtained is compared with the function $\alpha(q)$ numerically computed in the annealed approximation (equation 19).

Most of our simulations have been performed on systems with connectivity $K = 3$.

The agreement is very good when l , the temporal distance between the configurations, is large (in fig. 3 (b) data are shown for $l = 62$, in networks with $K = 3$ and $N = 50$), while the shape of the distribution is different, especially close to $q = 1$, for small values of l (in fig. 3 (a) we show data for $l = 2$, in networks with $K = 3$ and $N = 50$).

In the frozen phase the agreement between the annealed approximation and our data worsen. We simulated systems with $K = 2$ and different values of N . We show in figure 4 the function $\alpha(x)$ computed numerically within the annealed approximation and the one measured in the simulation with $N = 90$ using formula (48) (in this case, we subtracted the log term also for $q = 1$, because we expect $P(1)$ to be proportional to $1/\sqrt{N}$).

The agreement between data and computation is again better when the temporal distance between the configurations compared is large, but the real distribution is always much broader than the annealed one and the small overlap values are much more likely in the simulation than in the annealed approximation.

Then we tried to see if the overlap between configurations on the limit cycles is statistically different from the overlap between transient configurations. For such purpose we computed the function $\alpha_l(q)$ imposing two kind of conditions: on one hand, that both configurations be on the cycle, on the other that both configurations be transient.

In the chaotic phase (we report data with $K = 3$ and $N = 50$) the functions so obtained fit within one or two standard deviations (which are large, because the selection of trajectories is very severe) to the annealed prediction, for the same values of parameters for which the overall distribution gives a good function $\alpha(q)$, and so we don't see differences in the overlap distribution between pairs of transient configurations and pairs of configurations in the limit cycles.

The situation is different in the frozen phase where one can see that the most probable value of the overlap between transient configurations is quite lower than the most probable overlap between configurations of a cycle.

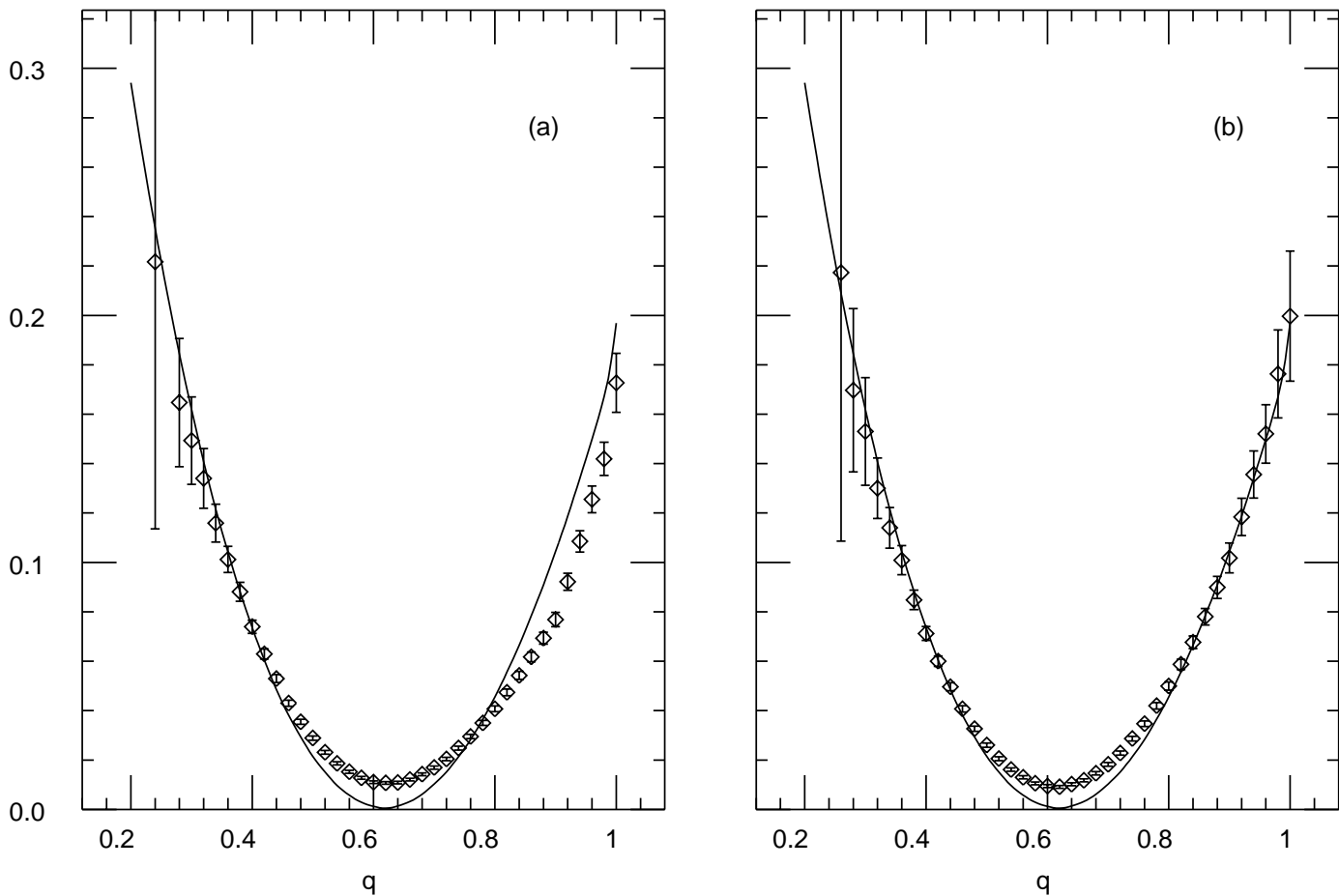


Figure 3: The function $\alpha_l(q)$, which is the exponential part of the distribution of the overlap $q(t, t + l)$. The solid line is the annealed prediction, the points plotted come from the simulation of 20000 networks with $K = 3$ and $N = 50$. The distribution is obtained considering different values of t between 50 and 80. (a): $l = 2$; (b): $l = 62$ (in this case the agreement for q close to 1 is much better). The condition that the trajectory must not be closed at time $t + l - 1$ selects respectively 79 and 63 per cent of trajectories in the sample.

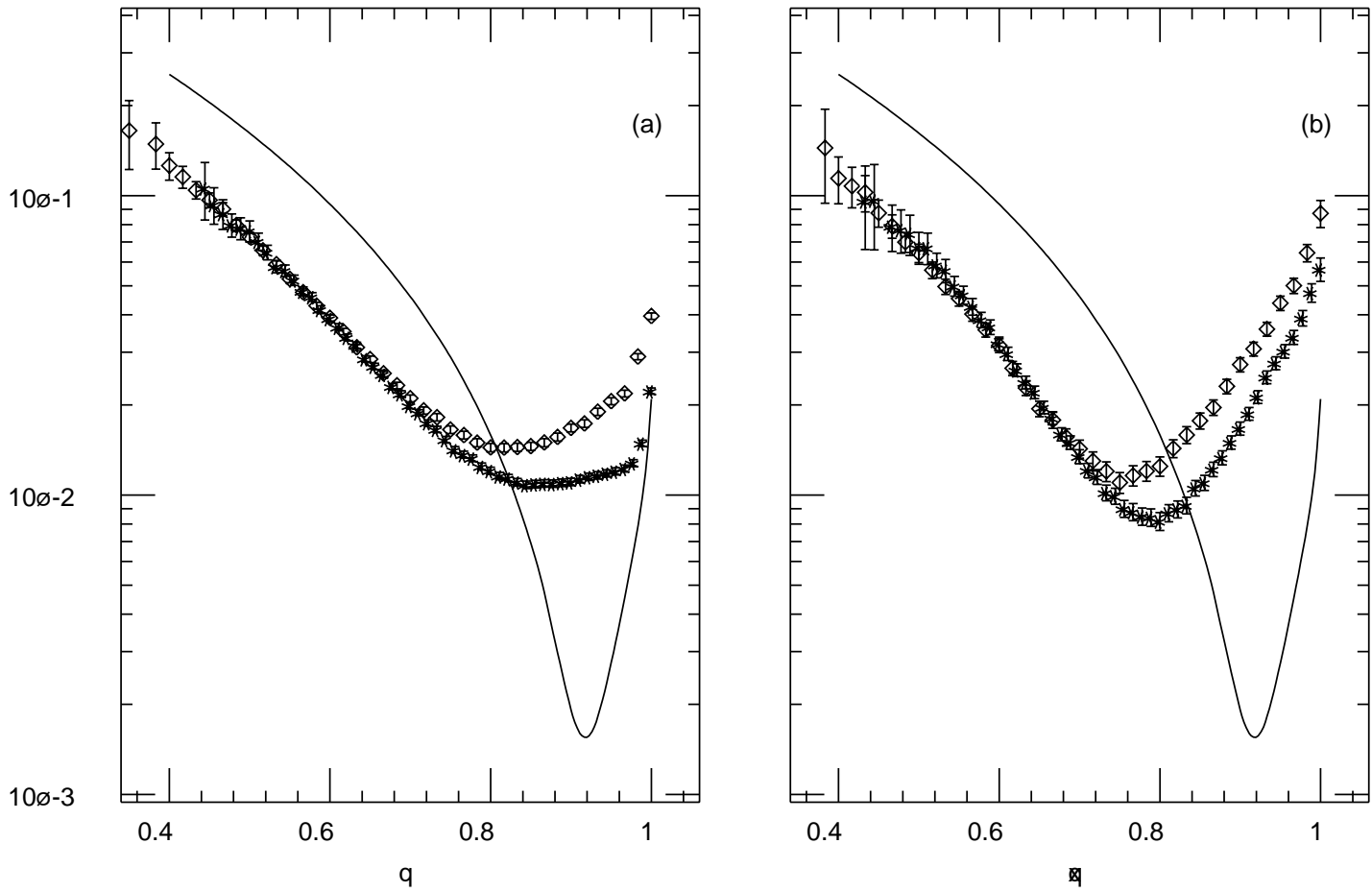


Figure 4: The function $\alpha_l(q)$, which is the exponential part of the distribution of the overlap $q(t, t+l)$. The solid line is the annealed prediction for $K = 2$ and $N = 90$, the points plotted come from the simulation of 40000 networks with $K = 2$, and N respectively equal to 60 (diamonds) and 90 (asterisks). The distribution is obtained considering different values of t between 12 and 20. The vertical scale is logarithmic. (a): $l = 2$; (b): $l = 26$. The condition that the trajectory must not be closed at time $t+l-1$ selects respectively 59 and 12.5 per cent of trajectories in the sample for $N = 60$ and 76 and 19 per cent for $N = 90$.

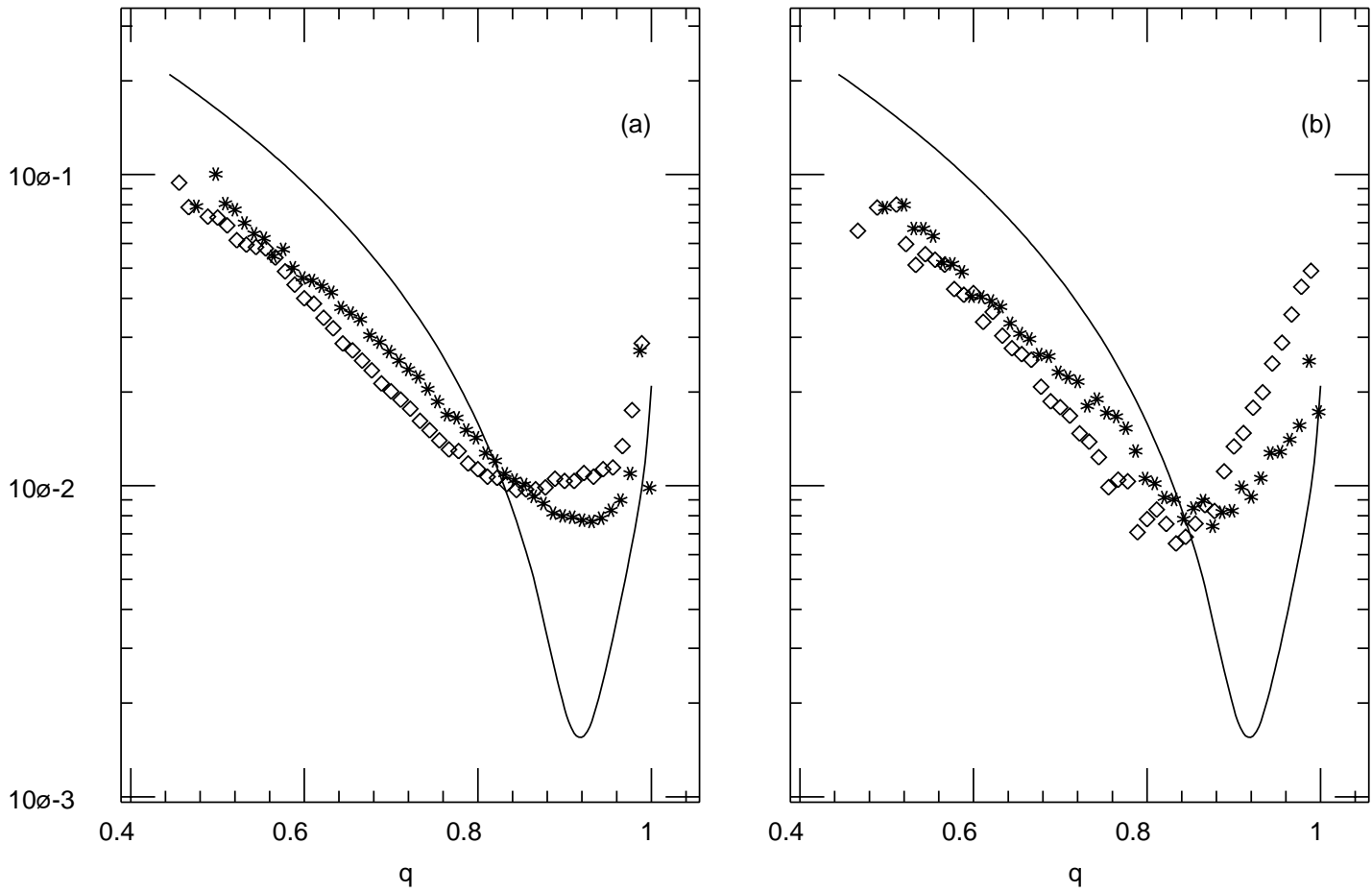


Figure 5: The function $\alpha_l(q)$ again. Here $K = 2$ and $N = 90$. The solid line is the annealed prediction, the points plotted come from the simulation of 40000 networks. The distribution of the overlap $q(t, t+l)$ is obtained considering different values of t between 12 and 20. The vertical scale is logarithmic. The two graphs concern $l = 2$ (a) and $l = 14$ (b) respectively. The asterisks are referred to the overlap of two configurations in a limit cycle, the diamonds to the overlap between transient configurations.

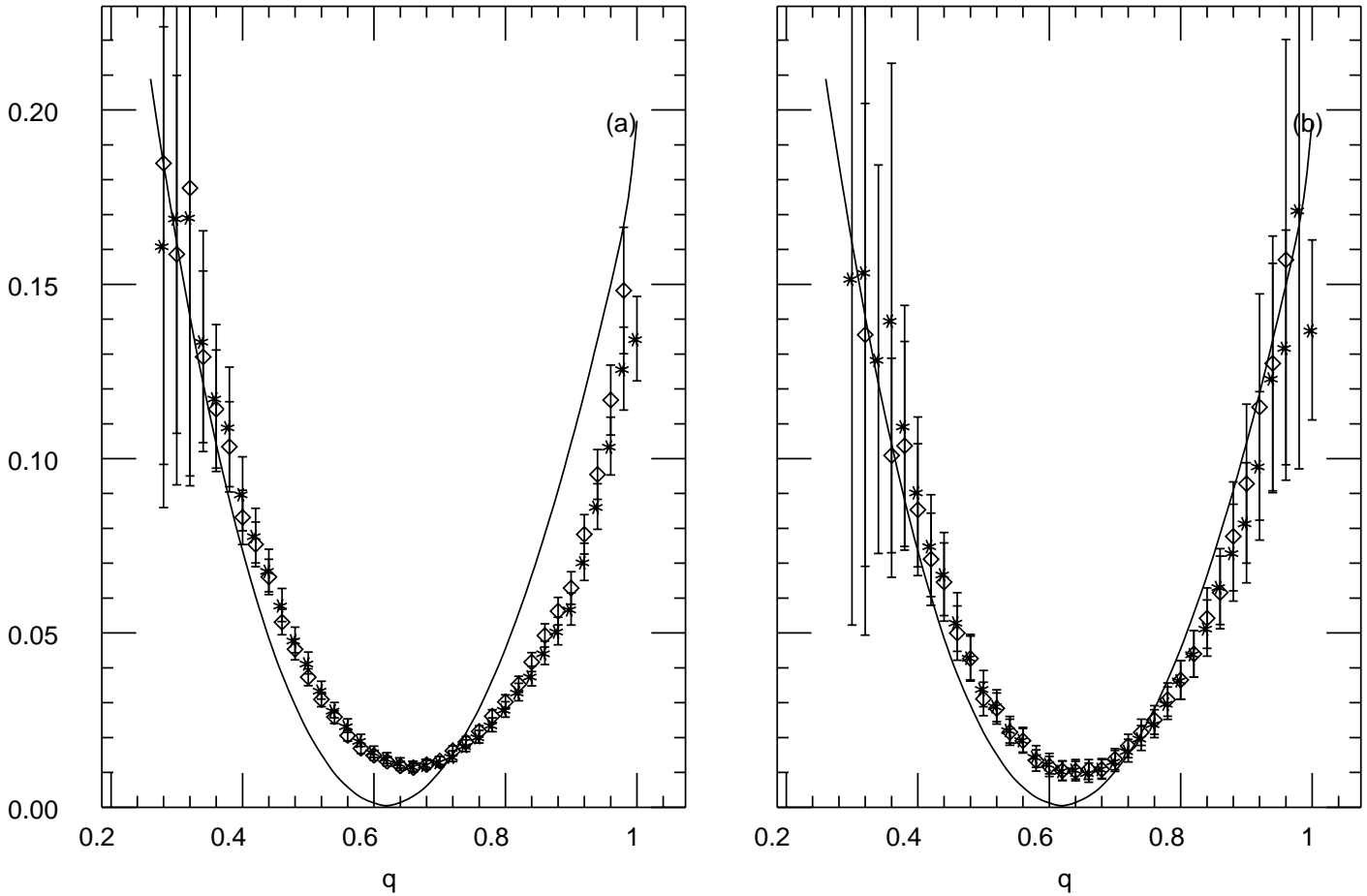


Figure 6: *The function $\alpha_l(q)$ again. Here $K = 3$ and $N = 50$. The solid line is the annealed prediction, the points plotted come from the simulation of 20000 networks. The distribution of the overlap $q(t, t + l)$ is obtained considering different values of t between 50 and 80. The two figures are concerned with $l = 2$ (a) and $l = 62$ (b) respectively. The asterisks are referred to the overlap of two configurations in a limit cycle, the diamonds to the overlap between transient configurations.*

7.2 Measure of the closing probabilities

In section 2 we defined the closing probability $\pi_N(t, t+l)$ as the probability that the configurations at times t and $t+l$ be equal, with the condition that the trajectory is not yet closed at the previous time steps.

We studied the closing probability for l fixed as a function of t , and we saw that in the quenched model the overlap distribution doesn't go to a stationary distribution as it is predicted by the annealed approximation.

For a fixed system size, the closing probability grows to a maximum value, usually larger than the annealed stationary value (but this depends on l !) and after it is always decreasing.

The rate of decrease appears to be independent on l , while the maximum value attained is not: it is larger if l is even and decreases with l for a given parity.

In figure 7 we report data for $K = 2$, which, in our case $\rho = 0.5$, is the starting point of the frozen phase, and $K = 3$ in the chaotic phase.

The simulation results are compared to the annealed closing probability exactly computed iterating equation (7). The time behaviour is at first in good agreement (especially for l large), over a fairly large range: in the networks with $K = 2$ and $N = 120$ the annealed and the quenched grow together from 10^{-36} to 10^{-2} . After, the annealed remains constant while the quenched decreases.

On the other hand, when we compared to the annealed approximation the closing probability measured at fixed times varying system size, we found out that the agreement, at the beginning not very good (many standard deviations), becomes very satisfactory taking larger systems.

Put into a graphic, the N behaviour of the closing probability appears to be an exponential decay with small corrections.

We now study the integral closing probability, $\tilde{\pi}_N(t)$, which is the sum over t' of $\pi_N(t', t)$. As usual, we considered two values of K , 2 and 3, in and near to the frozen phase, and N ranging from 60 to 180 for $K = 2$ and from 20 to 50 for $K = 3$.

Also $\tilde{\pi}_N(t)$ has a non monotone behaviour for t not too large: it increases to a maximum value and then start decreasing. Of course, it has to increase at large times, because it has to fulfil the normalization condition $\tilde{\pi}(2^N) = 1$, but in our simulations it keeps decreasing at all times accessible to measurement. In the framework of the annealed approximation, we expect that it grows linearly with t .

There is nothing new in this behaviour, which is just a consequence of the decrease in time of the closing probability, but it is the origin of other interesting features of the quenched system. In a next subsection we shall try to give an interpretation to this funny result, which is in contrast with the annealed approximation.

We show the temporal behaviour of $\pi_N(t)$ for different system sizes in the chaotic phase (fig. 9) and in the frozen one (fig. 8). The two plots have qualitatively the same shape, but in the frozen phase the integral closing probability decreases very slowly with system size

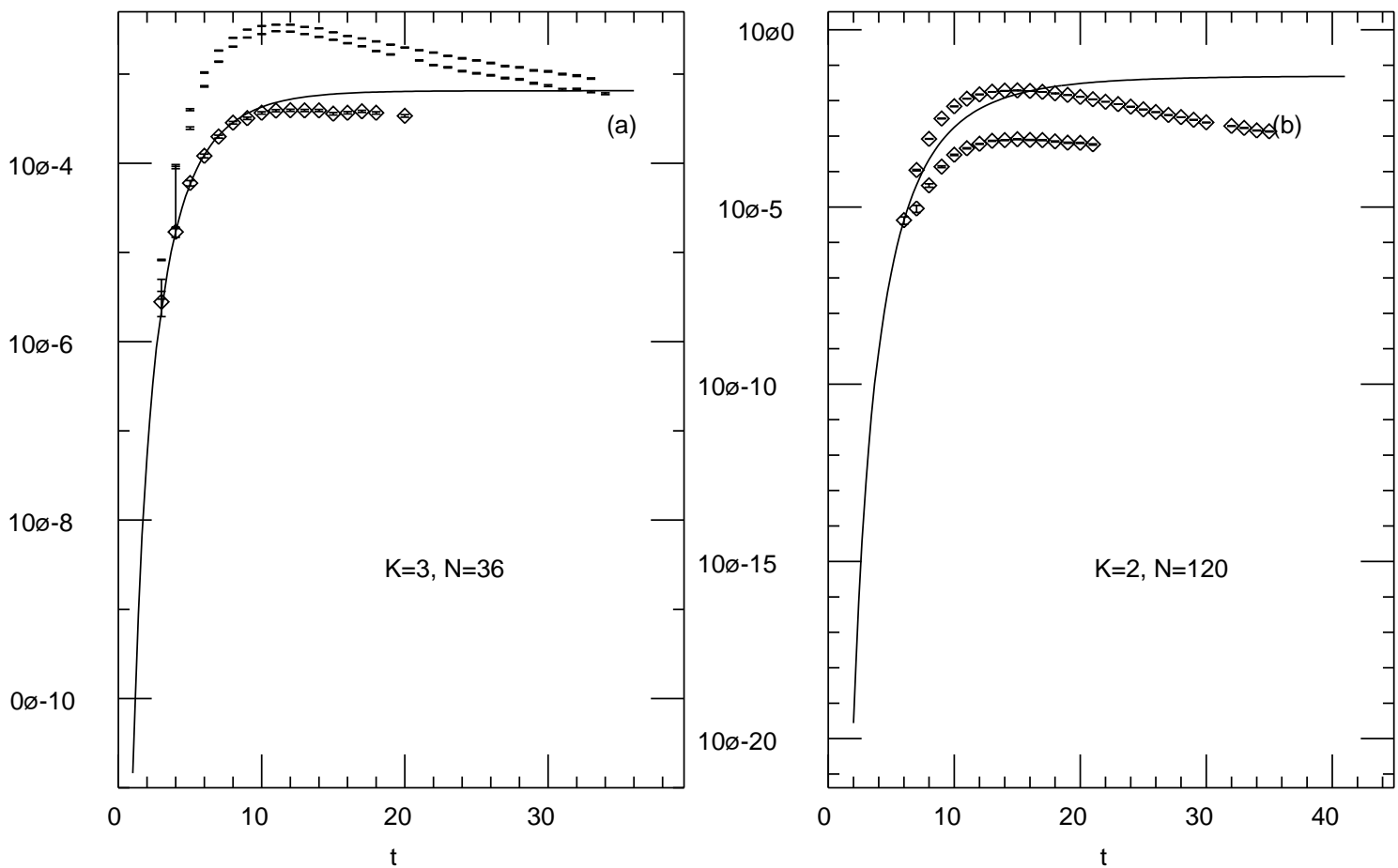


Figure 7: Closing probability $\pi_N(t, t+l)$. In solid it is reported the annealed value with $l=1$. The ordinate scale is logarithmic. (a): The system is in the chaotic phase, $K=3$ and $N=36$. Data correspond to $l=1$ (middle), $l=2$ (upper line: the closing probability is systematically higher) and to $l=15$ (diamonds; the agreement with the annealed approximation is better). (b): The system is at the critical point, $K=2$ and $N=120$. Data correspond $l=2$ (upper line) and to $l=15$ (diamonds). The first point of the annealed computation, $P = 7.52 \cdot 10^{-37}$, is not shown.

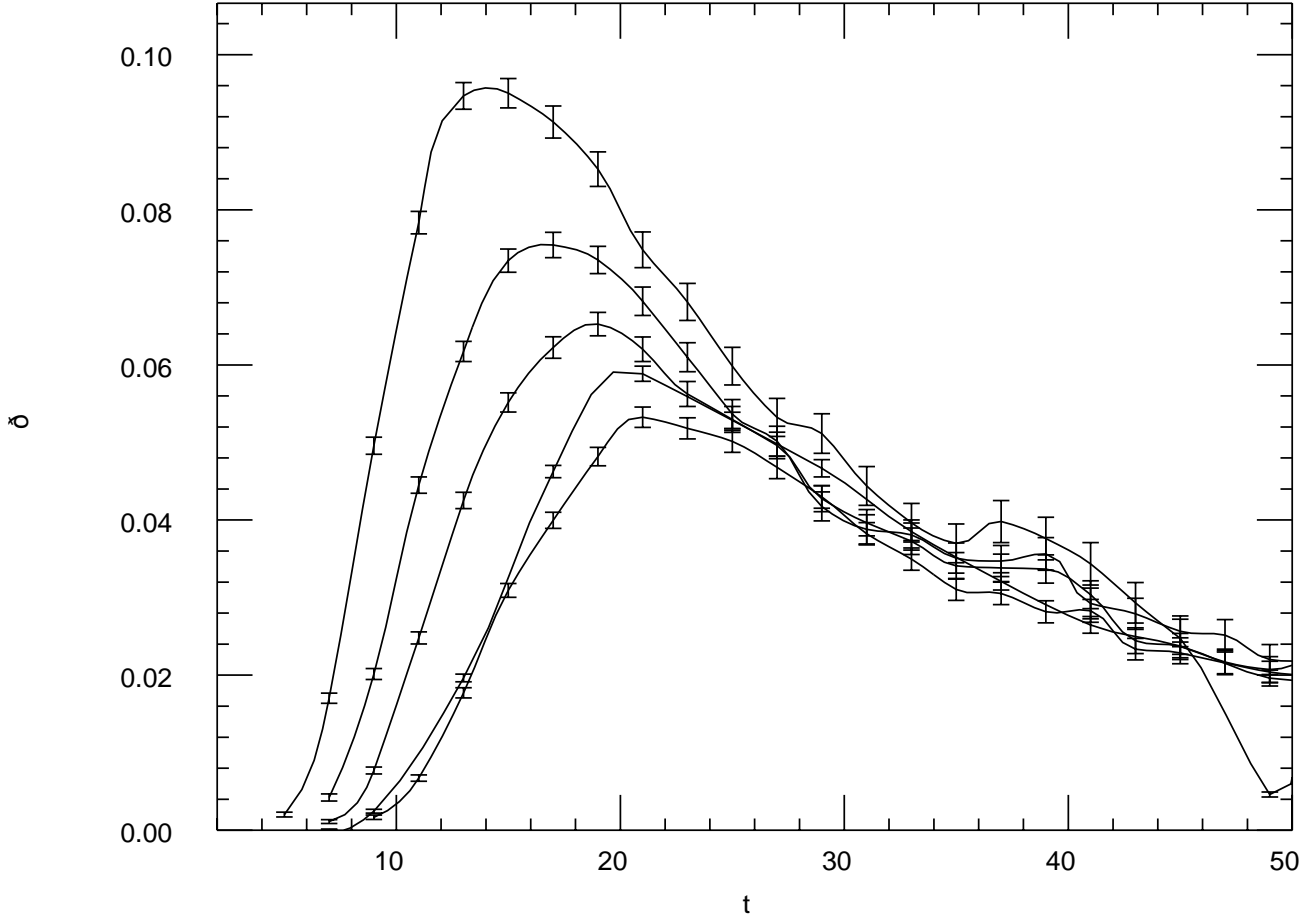


Figure 8: *Integral closing probability, $\tilde{\pi}_N(t)$ in the frozen phase ($K = 2$) for different system sizes: $N = 60, 90, 120, 150, 180$. $\tilde{\pi}_N$ reduces when N grows.*

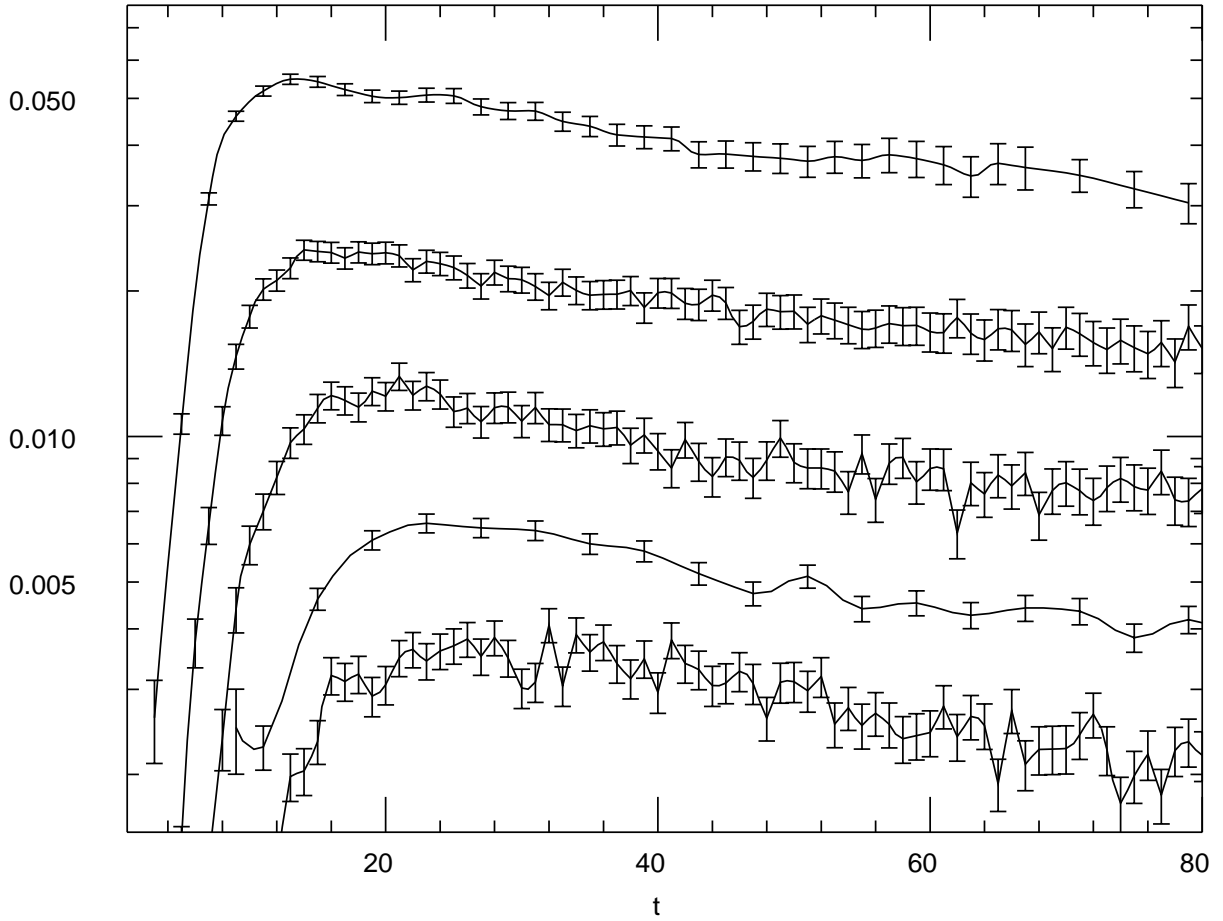


Figure 9: *Integral closing probability, $\tilde{\pi}_N(t)$ in the chaotic phase ($K = 3$) for different system sizes: $N = 20, 30, 40, 50, 60$. $\tilde{\pi}_N$ reduces when N grows.*

N , while in the chaotic phase it decays exponentially.

We also measured the mean overlap between successive configurations, $\bar{q}(t, t+1)$, without limiting the sample to the only trajectories not yet closed. We considered three different connectivities in the chaotic phase ($K=3,4$ and 5) and varied N .

As a function of t , this quantity increases to a stationary value which tends, when N grows, to the same value Q^* computed within the annealed approximation, but the (positive) corrections are large even for system sizes of the order of hundreds; on the other hand, when the temporal distance between the configurations compared is large, the corrections are much smaller.

This measurement was done without imposing the opening condition. When we measured the mean overlap between successive configurations, $\bar{q}(t, t+1)$, on the subset of the trajectories not yet closed at time $t+l$, we noticed that this quantity has a non monotone behaviour. It starts at $t=0$ with the value 0.5 , then increases, reaches a maximum value at about the same time at which the integral closing probability has its maximum value, and decreases again. Thus, the behaviour of the mean overlap parallels that of the closing probability.

This behaviour indicates that the condition that the trajectory is not yet closed at a certain time selects, from a point on, smaller and smaller overlaps. Fig. 11 shows the mean and the variance of the distance $d = 1 - q$ of successors on trajectories not yet closed and the integral closing probability for $K = 2$ and $N = 90$. The effect is more evident in the frozen phase, but it is still present in the chaotic phase for low values of K .

7.3 Properties of the cycles

Our simulations confirm well the predictions of the annealed approximation concerning the time scale of the period and of the transient distribution.

In the chaotic phase these quantities have an exponential behaviour, $\exp(\alpha N/2)$. We simulated systems with K ranging from 3 to 6 and several values of N (from 10 to 100 for $K = 3$, from 16 to 40 for $K = 4$, from 16 to 31 for $K = 5$ and from 6 to 28 for $K = 6$), generating at least 10000 samples of each network and few configurations on each network (except for the case $K = 3$, where we generated hundreds of initial configurations in order to compare the variance of cycle length on a given network with the variance between different networks).

We fixed a maximum time for the simulation, exponentially increasing with N ; in such a way, we underestimated the average cycle length because some trajectories were left before they completed their limit cycle; they were about one percent in the worst cases, but we think that this does not affect very much the determination of the exponents of the average period.

In fig.12 we plot the exponents α of the time scale of the system, defined by $\tau = \exp(\alpha N/2)$, and compare it with the annealed prediction, numerically computed.

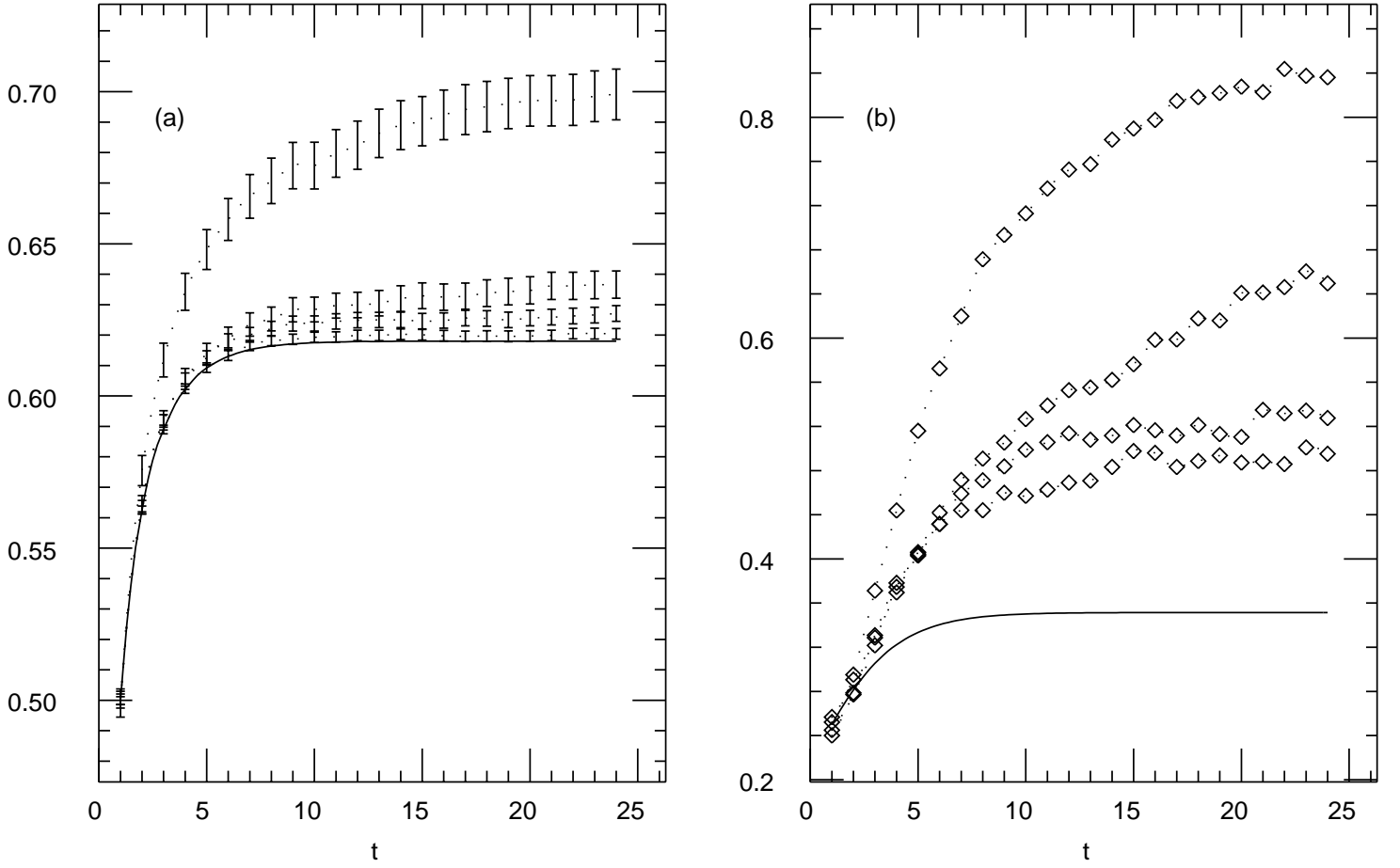


Figure 10: (a): Average overlap between successive configurations. The solid line shows the annealed equation, $Q(t+1) = \frac{1}{2}(1 + Q(t)^K)$. (b) Variance of the overlap between successive configurations. The solid line shows the annealed equation, $V(t+1) = Q(t+1)(1 - Q(t+1)) + \left(\frac{K}{2}Q(t)^{K-1}\right)^2 V(t)$. The system is in the chaotic phase, $K = 3$; data are shown for $N = 30, 80, 200$ and 400 ; the larger is N , the lower is the curve.

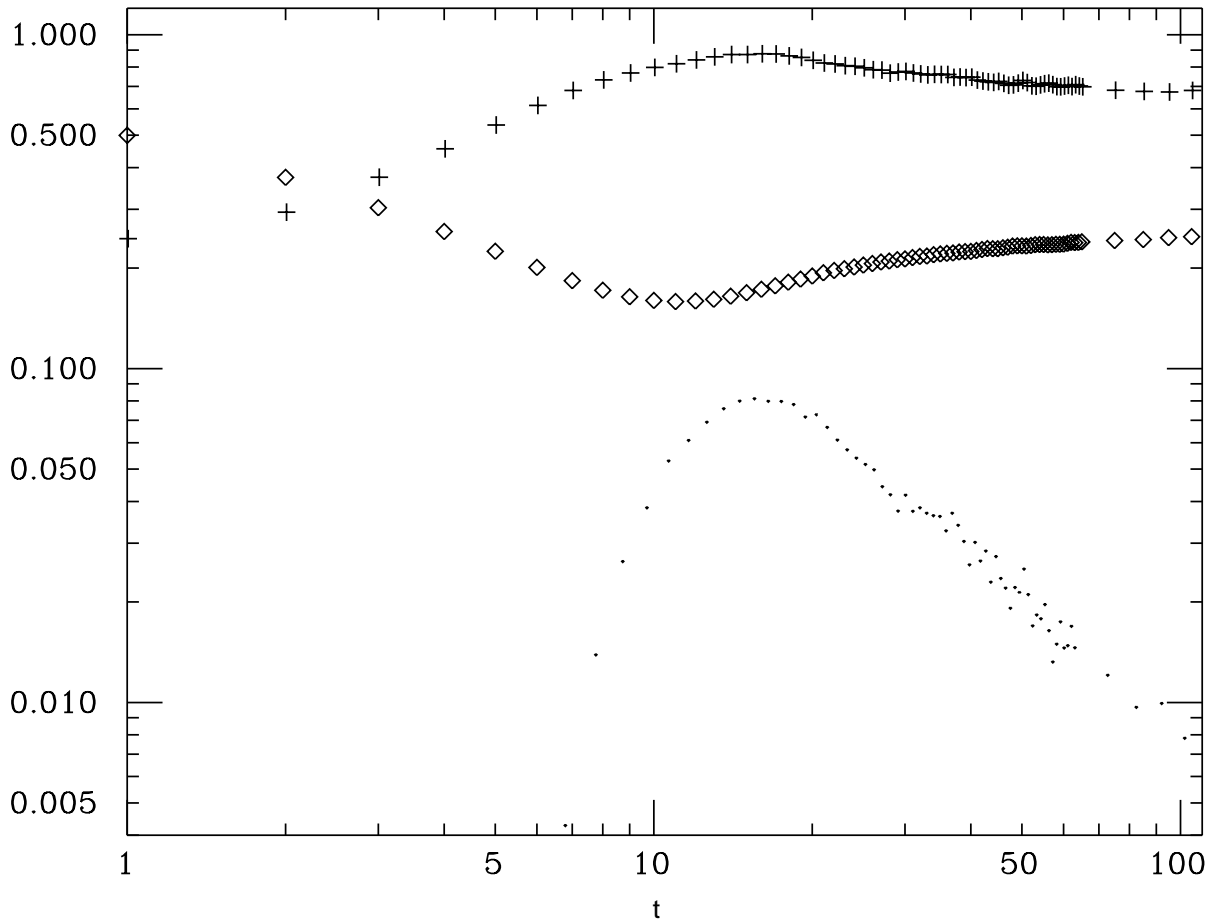


Figure 11: Average (\diamond) and variance (+) of the distance $d = 1 - q$ between successive configurations on trajectories not yet closed at time $t - 1$, as a function of t . It is also shown the integral closing probability, $\tilde{\pi}_N(t)$ (\cdot). $K = 2$, $N = 90$, 10000 sample networks.

It is possible to measure in the simulations four different exponents: α_L (twice the mean period exponent), α_V (the exponent of the variance of the period), α_T (twice the mean transient exponent), and α_P , the exponent of the time-scale of the period distribution (defined by fitting the probability to find a period larger than t with the function $\exp(-(t/\tau)^\beta)$).

These exponents were obtained through a fit of data with different N values. Their values lie very close within a few percent. In the figure there are not error bars, because the fits of our data are affected by finite size effects whose importance is difficult to estimate, but the agreement is quite good, even with not very large systems.

The largest deviation was found for the case $K = 3$, where the annealed approximation gives $\alpha = 0.182$ while our simulations give $\alpha_L = 0.210$, $\alpha_T = 0.204$, $\alpha_P = 0.21$ and $\alpha_V = 0.206$ for the average variance in a given network and 0.205 for the variance between different networks.

In this case, we performed the annealed computation with the map (19) and the same values of N used in the simulations, in order to obtain the corrections due to the discretization, whose effect is to increase α . In figure 13 we compare twice the logarithm of the average period (diamonds) with $N\alpha(N)$, where $\alpha(N)$ is computed with the annealed approximation. The discrepancies now are reduced respect to the asymptotic α value, but the simulation data still seem to be systematically larger and the angular coefficients are different.

In the simulations with $K = 3$ we measured also $F_N(t)$, defined in the second section as the probability that a random chosen trajectory is not yet closed at time t , and related to the closing probability by formula (4). According to the annealed approximation, one should find $\log(F_N(t)) \propto t^2$, because the closing probability reaches a constant value. In fact one finds that this quantity is linear or less than linear in t , so that $F_N(t)$ has a stretched exponential behaviour.

This feature is not surprising because we have already seen that the integral closing probability is a decreasing function of t from a point on, and $\log(F_N(t))$ is just its integral, but it is striking that the exponent of t is a slightly decreasing function of N .

This last observation was made looking at the period distribution which is a quantity much easier to compute: to measure $F_N(t)$ one has to keep in memory the whole trajectory, while to measure the period one needs only a reference configuration.

The distribution of cycle length L and transient time T are simply related to $F_N(t)$:

$$\text{Prob}\{T = t, L = l\} = F_N(t+l)\pi_N(t, t+l). \quad (49)$$

For $K = 3$, the probability to find a cycle of period greater than t decays as a stretched exponential, $\exp(-(t/\tau)^\beta)$; the time scale τ grows exponentially with N , with the same exponent α_L of the average cycle length; the decay exponent β goes down with N , even if very slowly: we found an exponent of 0.91 for $N = 10$ and 0.39 for $N = 100$. This fact is in contradiction with the results of the annealed approximation, which predicts $\beta = 2$, but it is a direct consequence of the decreasing with time of the closing probability.

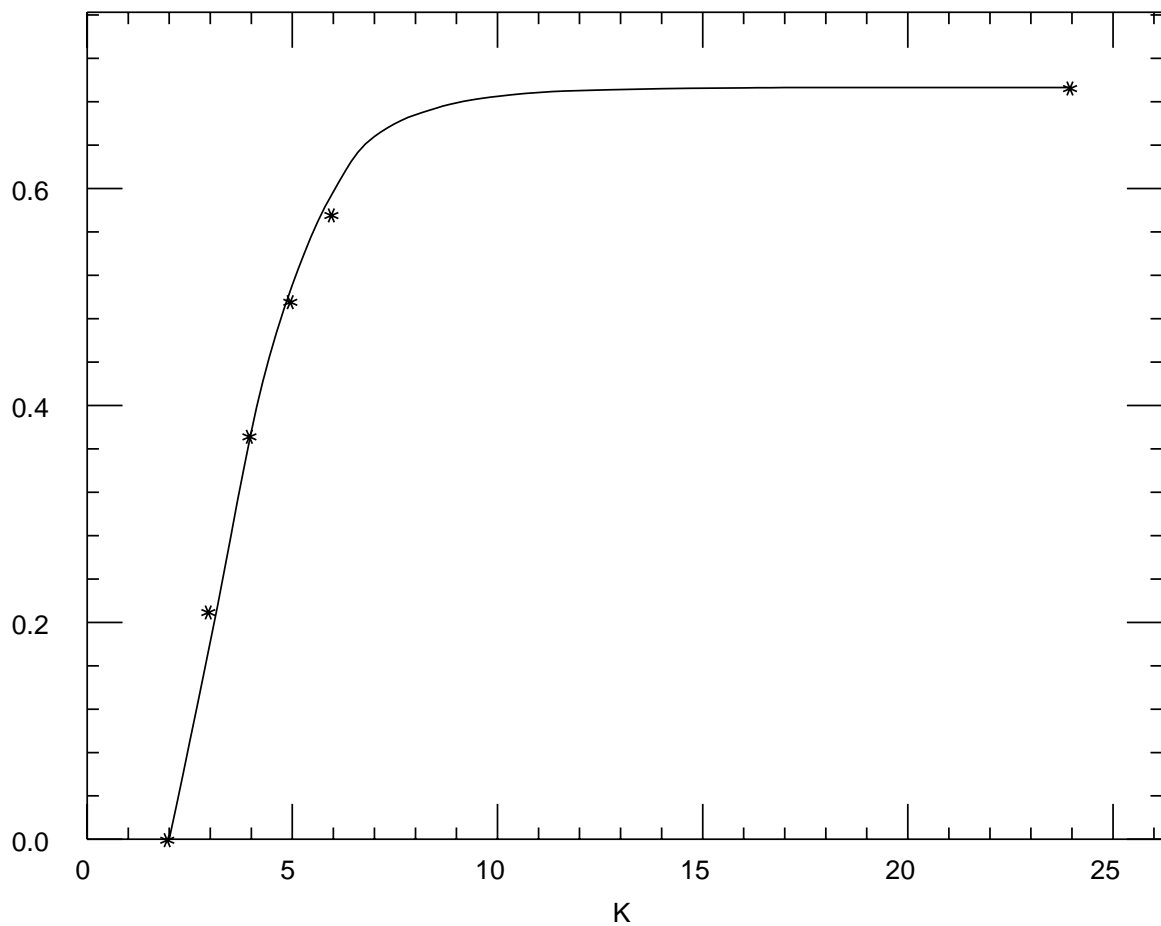


Figure 12: *The function $\alpha(K)$, where α is twice the exponent of the characteristic time-scale of period and transient distribution, $\tau = \exp(\alpha N/2)$, for $\rho = 0.5$, as obtained from the annealed approximation. The asterisks are obtained from a fit of simulational data; the last one is the theoretical result for the Random Map.*

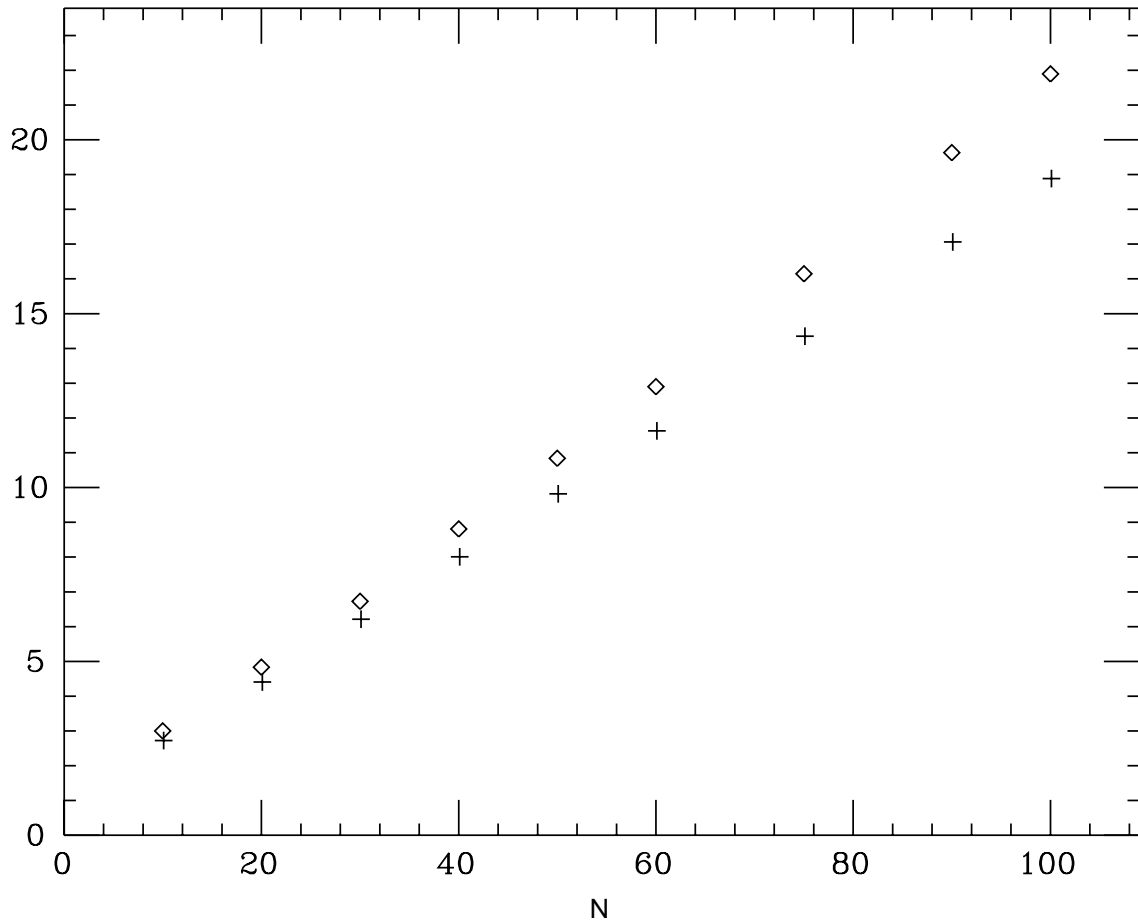


Figure 13: (\diamond) : twice the logarithm of the average period in networks with $K = 3$ and N nodes (simulation); (+) : the annealed coefficient α computed in the saddle point approximation for a system of N nodes, times N .

From our simulations on systems with $K = 2$ and N ranging from 30 to 90 and $K = 3$ and N ranging from 10 to 100 it appears that the histogram of transient time has a peak corresponding to the time t where the closing probability reaches its maximum value, and then decreases as a stretched exponential; and the cycle length histogram decreases with the same law.

In addition, very short periods are much more common respect to the others than one would expect on the basis of the annealed approximation (see figure 14).

Another unexpected feature of the period distribution is the fact that cycles of even lengths are more likely than odd ones, as one can already see by the fact that the closing probability is higher for even periods.

We have seen in this fact a clue of a non trivial distribution of local periodes, say the period of a single element in a network. We have obtained in our simulations an indirect confirmation of this guess. We will present these data in a forecoming paper.

8 Discussion

In this work we used a stochastic scheme, generalizing the analysis by Derrida and Flyvbjerg of the Random Map Model to finite values of K , in order to compute the distributions of cycle lengths, transient times and attraction basins weigths in Kauffman Networks. The definition of the closing probabilities is crucial in this scheme.

The annealed approximation, introduced by Derrida and Pomeau, has revealed to be a good tool for the computation of the closing probabilities and the approximate solution of the model.

There are deviations from the approximation, which are larger close to the frozen phase, but the mean quantities that we computed are in good agreement with our numerical results. The annealed approximation works better in the chaotic phase, but it allows also to predict an universal behaviour of cycle lengths along the critical line. We have in plan to check this point.

We haven't, till now, tried to justify the approximation used. The annealed approximation allows to compute the overlap distribution using only a minimal information about the past evolution of the system and neglecting everything else, so we think that a loss of memory of the history of the system is needed for its validity. This fact is consistent with our numerical results, which show that the overlap of two configurations very far apart along the trajectory is in some sense "more annealed" than the overlap of two configurations temporally closer. How this loss of memory comes about and what are its limitations would be an interesting question to address to understand in a more analytical way dynamical systems with quenched disorder.

As we saw in the previous section, the main discrepancies between our simulations and the annealed approximation arise from the fact that the closing probabilities ultimately

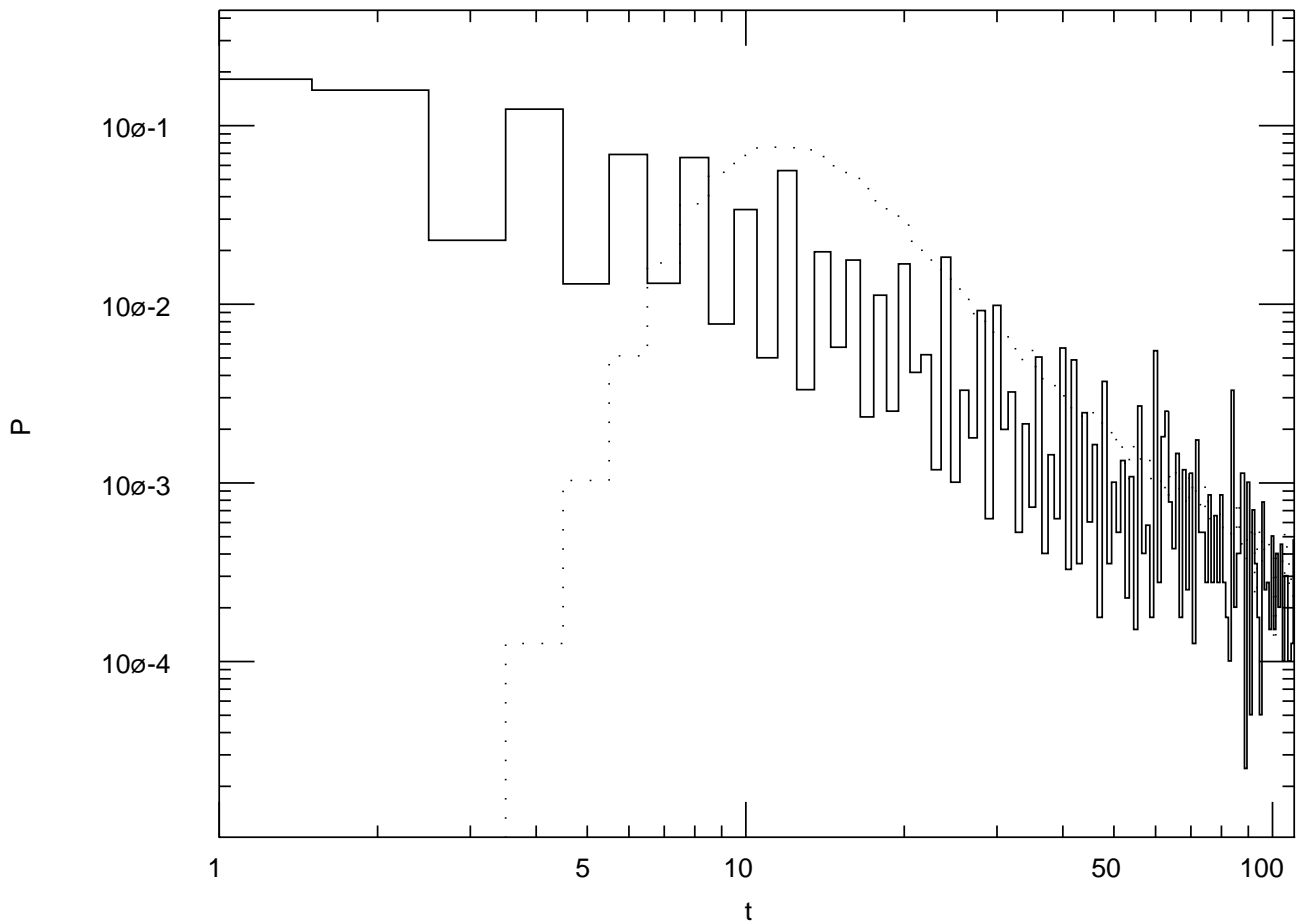


Figure 14: *Histogram of cycle (solid line) and transient (dots) length for a system in the frozen phase, $K = 2$ and $N = 120$. 10000 sample networks were generated.*

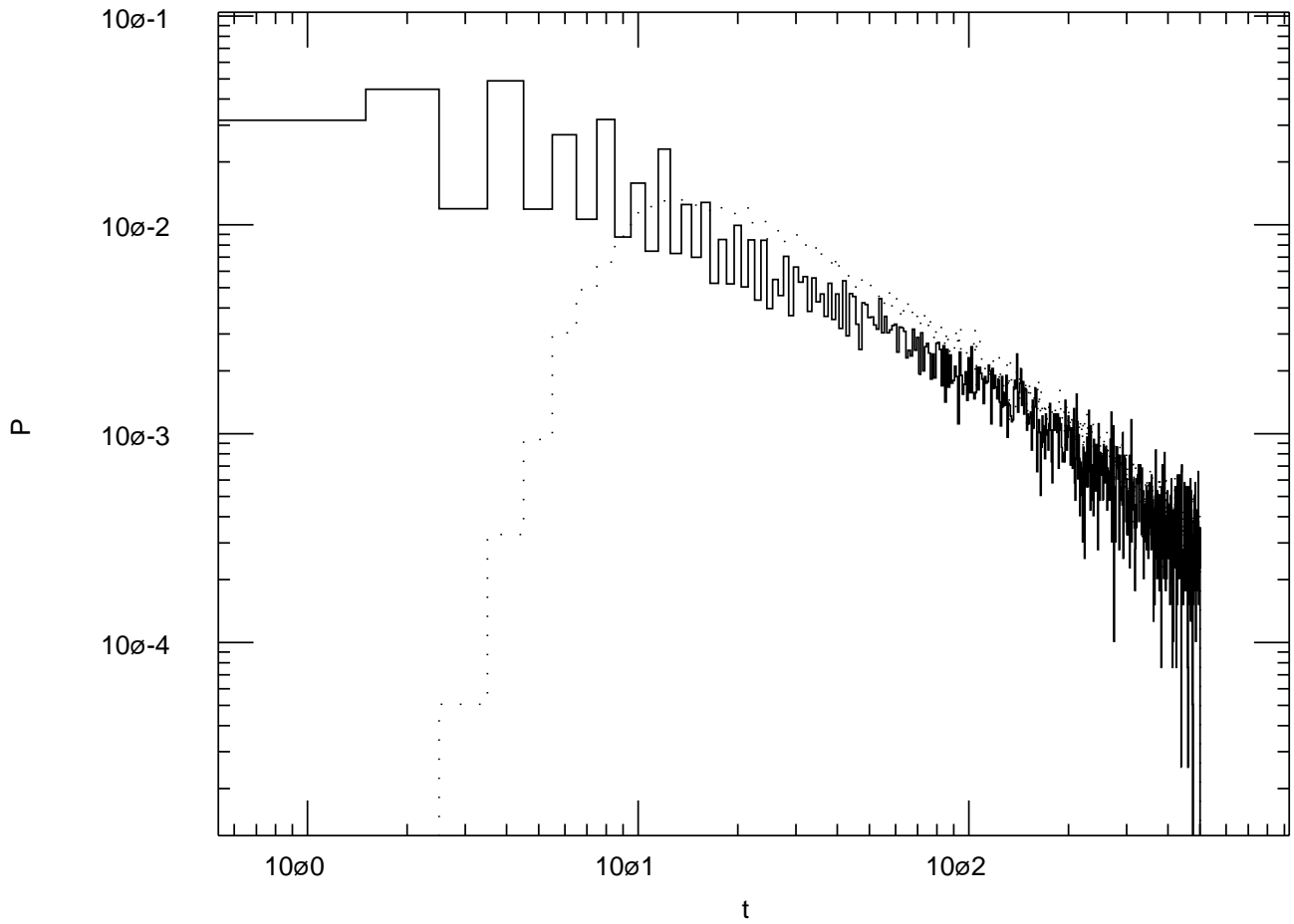


Figure 15: *Histogram of cycle (solid line) and transient (dots) length for a system in the chaotic phase, $K = 3$ and $N = 50$. 10000 sample networks were generated.*

decrease in time.

This fact can be interpreted as a consequence of the definition of the closing probabilities as conditional probabilities: the requirement to consider only trajectories not yet closed selects, from a time on, trajectories where the typical overlaps are smaller and smaller.

We did not impose the opening condition in our computation, so we think that the best way to improve the annealed approximation would be to take into account the opening of the trajectory in the computation. This purpose requires to keep memory of much more information about the past history of the trajectory than the simple one that we used in doing the annealed computation. We are planning to try to do this in a next work.

9 Acknowledgments

We thank Bernard Derrida for a stimulating discussion. Ugo Bastolla thanks Luca Peliti and Henrik Flyvbjerg for interesting discussions and for reading the manuscript.

References

- [1] S.A. Kauffman (1969), Homeostasis and Differentiation in Random Genetic Control Networks, *Nature* **244**, 177-178
- [2] S.A. Kauffman (1984), *Physica D* **10** 145
- [3] M. Mezard, G. Parisi, M.A. Virasoro (1987), *Spin Glass Theory and Beyond*, Singapore: World Scientific
- [4] Derrida B. and Y. Pomeau (1986), Random Networks of Automata: a Simple Annealed Approximation, *Biophys. Lett.* **1(2)**, 45-49
- [5] B. Derrida and H. Flyvbjerg (1986), Multivalley Structure in Kauffman's Model: Analogy with Spin Glasses, *J.Phys.A: Math.Gen.* **19**, L1003-L1008
- [6] B. Derrida, H. Flyvbjerg (1986), The random map model: a disordered model with deterministic dynamics, *Journal de Physique* **48**, 971-978
- [7] B. Derrida, D. Stauffer (1986): Phase Transitions in Two-dimensional Kauffman Cellular Automata, *Europhys. Lett.* **2(10)**, 739-745
- [8] H. J. Hilhorst and M. Nijmayer (1987), On the Approach of the Stationary State in Kauffman's Random Boolean Network, *J. Physique* **48**, 185-191

- [9] B. Derrida and H. Flyvbjerg (1987), Distribution of Local Magnetisations in Random Networks of Automata, *J.Phys.A: Math.Gen.* **20**, L1107-L1112
- [10] H. Flyvbjerg (1988), An Order Parameter for Networks of Automata, *J.Phys. A:Math.Gen.* **21** L955-L960
- [11] H. Flyvbjerg, N.J. Kjaer (1988), Exact Solution of Kauffman Model with Connectivity One, *J.Phys. A:Math.Gen.* **21(7)**, 1695-1718
- [12] B. Derrida (1988), Dynamics of automata, spin glasses and neural network models, in: *Nonlinear evolution and chaotic phenomena*, Ed. G. Gallavotti and P.F. Zweifel, Plenum Publishing Co., 1988.
- [13] H. Flyvbjerg (1989), Recent results for random networks of automata, *Acta Physica Polonica B20*, N.4, p. 321.
- [14] S.A. Kauffman (1989), Principles of Adaptation in Complex Systems, in: *Lectures in the Sciences of Complexity*, SFI Studies in the Sciences of Complexity, Ed. D. Stein, Addison-Welsey Longman, 1989.
- [15] S.A. Kauffman (1990), *Origins of Order: Self-Organization and Selection in Evolution*, Oxford University Press

